Nucleation Limitation and Hardenability

R. C. SHARMA AND G. R. PURDY

The relation between nucleation theory and hardenability of steels has been critically examined. The effect on hardenability of most elements with the exception of boron and strong carbide forming α-stabilizers, is found to be semiquantitatively consistent with classical nucleation theory. The "anomalous" effects of boron, chromium and molybdenum, are discussed in terms of possible physical interference of precursor reactions with ferrite formation.

THE relationship between nucleation theory and hardenability remains a challenging topic for scientific investigation. The early reviews of Hobstetter[1] and Christian[2] and the recent and comprehensive review by Russell[3] provide much of the source material for this work. The purposes of this contribution are:

1) To use the general theory to draw some broad inferences about nucleation effects in hardenability.

2) To formulate explicitly the thermodynamics of nucleation in three component systems (the minimum number of components which permits the term "hardenability" to take its full meaning).

3) To compute relative hardenability effects of selected alloying elements.

4) To compare the orders-of-magnitude of nucleation times and alloying element effects with those expected on the basis of classical heterogeneous nucleation theory, and as a complement, to construct a plausible model for the critical nucleus for proeutectoid ferrite in austenite.

5) To draw attention to alloy systems which depart from predictions of the elementary theory and to speculate on the causes of these departures.

THERMODYNAMICS OF NUCLEATION

The theory of thermally activated nucleation focusses on the (unstable) equilibrium between the critical nucleus (of phase α) and the parent phase (β). The interface is assumed to be sharp, and the precipitate and matrix are assumed to be uniform in composition. The free energy of the nucleus is a maximum with respect to growth or decomposition, and a minimum with respect to any other process, such as a change in shape or composition. It is this postulated unstable equilibrium which makes tractable the discussion of the effects of complex fluctuations at the submicroscopic level in terms of measurable macroscopic quantities.

Provided that the macroscopic quantities are precisely defined, it is possible to draw from the theory a number of illuminating statements about nucleation behavior. It should be noted, however, that the assumptions described above have been challenged by nearly every writer in the field of nucleation theory. While the assumption that macroscopic equilibrium properties obtain at the fluctuation stage can be justified by detailed arguments in many cases,[4] in regimes where the fluctuations are known to be coherent, and the interfaces are diffuse, classical nucleation theory fails conclusively. The reader is referred to the work of Cahn and Hilliard as recently reviewed by Hilliard.[5] More relevant to the present discussion is the case where the macroscopic interface contains defects which periodically interrupt coherency. If the spacing between defects (*e.g.*, dislocations) is greater than the nucleus size, then the assignment of macroscopic interface properties to the nucleus must be critically analyzed.

We will be concerned with the driving force for nucleation in multicomponent systems, ΔG_v, in energy per unit volume. In binary systems, this quantity is obtained from free energy vs composition curves by constructing a tangent to the parent phase free energy curve at the bulk composition, as in Fig. 1, and determining the vertical distance $V_\alpha \Delta G_v$ to the precipitate composition. This latter is obtained by constructing a second tangent to the precipitate free energy curve, such that $\Delta\mu_1 = -K\sigma_{\alpha\beta}\bar{V}_1^\alpha$ and $\Delta\mu_2 = -K\sigma_{\alpha\beta}\bar{V}_2^\alpha$, where K is curvature, $\sigma_{\alpha\beta}$ the interfacial free energy and V_i^α the partial molar volume of i in the precipitate (α). This is the Gibbs-Thomson equilibrium condition. The double tangent construction is due to Hillert,[6] and provides a useful and general graphical method for deter-

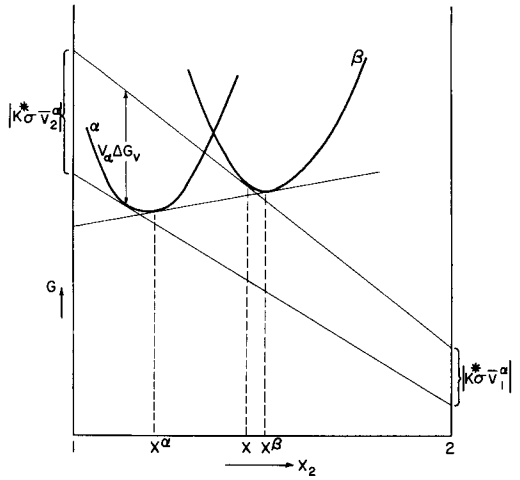

Fig. 1—Illustrating the equilibrium construction for α nuclei of critical size, i.e., with critical curvature K^*. The matrix composition is X and the most probable nucleus composition is that which maximizes ΔG. For comparison the infinite radius equilibria X^α and X^β are shown (after Hillert[6]).

R. C. SHARMA and G. R. PURDY and Graduate Student and Professor, respectively, Department of Metallurgy and Materials Science, McMaster University, Hamilton, Ontario, Canada. This paper is based on a presentation made at a symposium on "Hardenability" held at the Cleveland Meeting of The Metallurgical Society of AIME, October 17, 1972, under the sponsorship of the IMD Heat Treatment Committee.

mining phase equilibria involving curved interfaces in systems where partial molar volumes differ. This procedure is particularly important when an interstitial solute is involved. The more usual construction, *e.g.*, Fig. 2, from Hobstetter,[1] assumes equal partial molar volumes, and is approximate only.

For ternary systems this construction is easily extended, as described below. The Gibbs-Thomson equation is again:

$$\Delta\mu_i = -K\sigma_{\alpha\beta}\bar{V}_i^{\alpha}; \qquad i = 1, 2, 3. \qquad [1]$$

The driving force for nucleation is proportional to the vertical distance from the plane, which is tangent to the parent phase free energy surface at the bulk phase composition, to the precipitate free energy surface at the precipitate composition.

As suggested by this construction, the volume free energy change of nucleation of several phases (stable or metastable) in the ternary field may be appreciable, their rates of nucleation and order of appearance being determined by kinetic factors and surface energies as well as the relative magnitudes of ΔG_v.

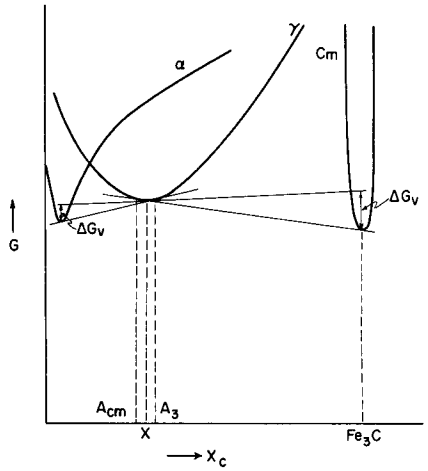

Fig. 2—For undercooled austenite (γ) of eutectoid composition the approximate driving forces for nucleation of ferrite and cementite are represented by the respective distances from tangent at X to the ferrite and cementite free energy curves (after Hobstetter[1]).

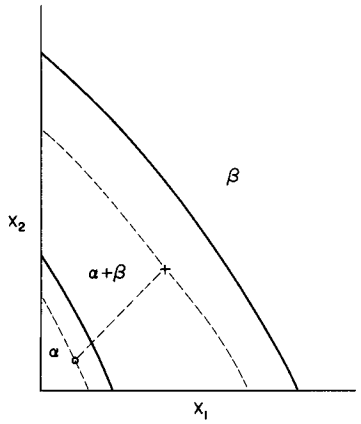

Fig. 3—The composition of the equilibrium critical nucleus (0) in the ternary system containing solutes 1 and 2 is given by the capillarity-modified tie-line which terminates at the bulk parent phase composition X. For dilute solutions, the solute distribution coefficients for critical curvature are independent, and related to the zero curvature solute distribution coefficients by Eqs. [2] and [3].

The composition of the critical nucleus in a ternary system is readily obtained from capillarity theory. For example, in the terminal portions of the ternary isotherm, which consist of dilute (noninteracting) solutes with distribution coefficients $k_i = C_i^{\alpha}/C_i^{\beta}$, we have the approximate expressions

$$k_1^* = k_1^0 e^{-K^*\sigma\bar{V}_1^{\alpha}} \qquad [2]$$

and

$$k_2^* = k_2^0 e^{-K^*\sigma\bar{V}_2^{\alpha}} \qquad [3]$$

where the superscript * refers to a distribution coefficient under critical curvature K^* and the superscript 0 refers to zero curvature. Since the matrix composition now lies on the phase boundary, as shown in Fig. 3, the critical equilibrium nucleus composition is uniquely determined by these two expressions. Of course, other compositions of nuclei may form, but with small probability unless kinetic parameters militate in their favor (see below).

This is the local equilibrium model for nucleation in three component systems. In the previous contribution, Coates[7] discusses two kinds of equilibrium models which can obtain during unpartitioned growth, including the local equilibrium no-partition (LE-NP) model. For nucleation, no parallel model exists; partition of alloying elements must accompany the formation of a true local equilibrium nucleus.

At large supersaturations, the possibility exists that unpartitioned nuclei may form, because of the great time required for alloying element redistribution. In this case, a special kind of partial equilibrium termed "paraequilibrium" by Hultgren[8] and Hillert,[9] (or the similar concept of "no-partition equilibrium" of Aaronson, Domian, and Pound[10]) may apply. Fig. 4 shows the paraequilibrium construction which assures equal activities of carbon in parent and product phases. Here the tie-line coincides with a component ray. A paraequilibrium diagram as modified by capillarity is given in

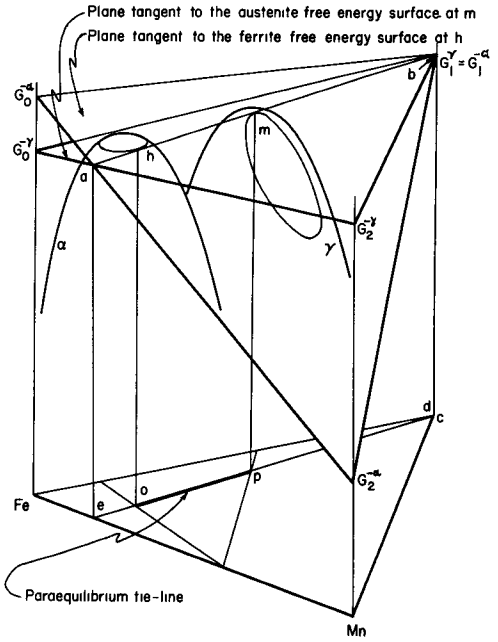

Fig. 4—Schematic free energy surfaces for ferrite and austenite illustrating the paraequilibrium conditions (after Gilmour, Purdy, and Kirkaldy[12]).

Fig. 5. A calculated paraequilibrium phase diagram is shown superimposed on a true ternary isotherm for Fe-C-Ni in Fig. 6.[11]

Note that, at low supersaturations, the host phase is not supersaturated with respect to the paraequilibrium boundaries, so that alloying element partition is necessary. At higher supersaturations, the formation of unpartitioned (or partially partitioned) nuclei is possible. For unpartitioned nuclei, the appropriate form of the Gibbs-Thomson equation is that given by Gilmour *et al.*[12] as

$$\mu_1^\alpha - \mu_1^\beta = -K\sigma_{\alpha\beta}\bar{V}_1^\alpha \quad [4]$$

$$\mu_2^\alpha - \mu_2^\beta + \frac{C_3}{C_2}(\mu_3^\alpha - \mu_3^\beta) = -K\sigma_{\alpha\beta}\left[V_2^\alpha + \frac{C_3}{C_2}\bar{V}_3^\alpha\right] \quad [5]$$

Here subscripts 1, 2, and 3 refer to carbon, the immobile solute and the solvent (iron), respectively. This expression is seen to reduce to the paraequilibrium condition for large radii.

The capillarity conditions given above also apply to precipitates with nonisotropic interface properties. In this case, the condition that the critical nucleus possesses the equilibrium shape will assure that σ_i/r_i is a constant,* which can be substituted directly into the capillarity equations.

*For interfaces in cusp orientations; r_i must be measured perpendicular to the interface plane.

Strain energy, whether associated with volume change, or with the maintenance of coherency, should be added to the ΔG_v term in the nucleation equations whenever it becomes significant.[3]

In any quantitative test of the applicability of nucleation theory to steels, the free energies of transformation must be known. Figs. 7 and 8 give our calculated values of these free energies for the alloy systems Fe-C-Ni and Fe-C-Mn for paraequilibrium and local equilibrium modes. We consider that the thermodynamics of these systems are among the most reliable available. Similar values of ΔG_v have been given for these and other alloy systems by Aaronson, Domian, and Pound.[10] symmetric spherical caps at grain boundaries, the contact angle being determined by the balance of interfacial free energies at the nucleus edge. They showed that grain boundaries can act as very effective nucleation catalysts. Recently, Russell[19] considered the nucleation of several types of grain boundary precipitates, including incoherent allotriomorphs, coherent (on one side) allotriomorphs and discs. He assumed that the coherent allotriomorph possessed one interface which was isotropic and of low energy (hence the equilibrium nucleus bulges into the grain with which the nucleus shares a favorable orientation relationship as shown in Fig. 9). The energetics of nucleation of these figures are developed by straightforward methods of classical nucleation theory, and are tabulated in Table I. Russell also obtained expressions for the incubation times, and these are also listed in Table I. To determine the incubation time the principle of microscopic reversibility[20] is invoked, and the dissolution of the subcritical cluster studied. For incoherent allotriomorphs, Russell con-

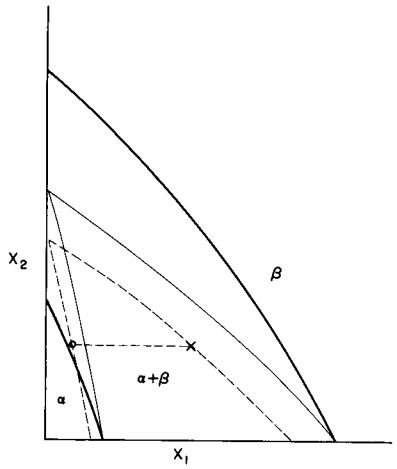

Fig. 5—The equilibrium phase diagram (heavy lines), and the paraequilibrium phase diagram (light lines) are compared. The capillarity-modified paraequilibrium boundaries for a critical nucleus (bulk parent phase composition X) are shown as broken lines. The broken tie-line joins the bulk matrix composition to the paraequilibrium (unpartitioned) nucleus composition (0).

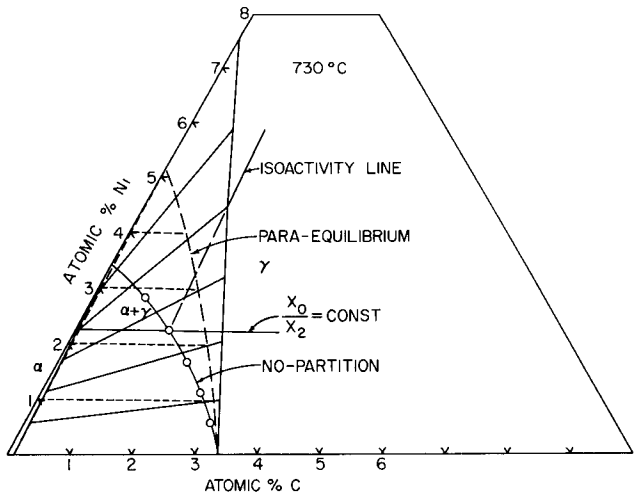

Fig. 6—Calculated isotherm of Fe-C-Ni at 730°C. Also shown are the paraequilibrium and no-partition boundaries for local equilibrium growth.

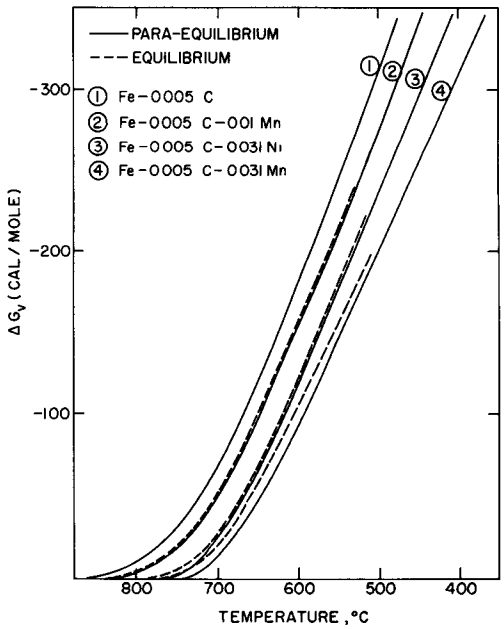

Fig. 7—Free energy for nucleation vs temperature for four 0.1 wt pct C alloys.

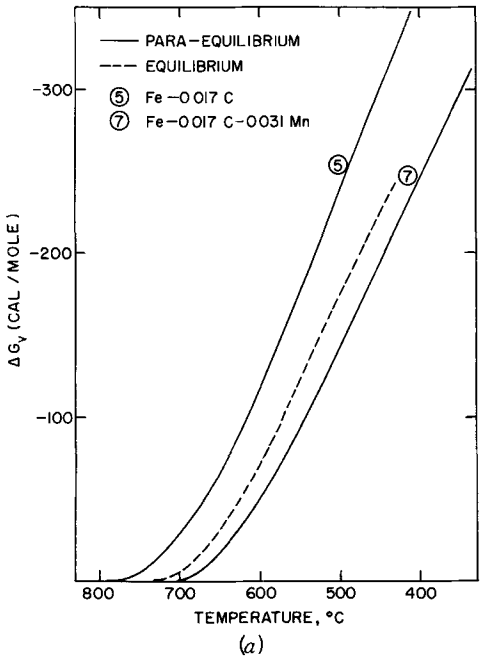

Fig. 8—(*a*) The effect of Mn on the free energy for nucleation of ferrite. (*b*) The effect of Ni on the free energy for nucleation of ferrite. Note that the unpartitioned and partitioned reaction have similar driving forces.

siders that interfacial solute diffusion controls dissolution, and the frequency factor β_k is estimated as the boundary jump frequency D^b_{eff}/a^2 multiplied by the number of solute atoms within one jump distance of the allotriomorph edge, *i.e.*,

$$\beta_k = \frac{\Pi r^* D^b_{\text{eff}} \sin\theta \bar{C}}{a^3} \qquad [6]$$

where a is the jump distance and $\bar{C}$ is the solute concentration in the matrix.

Now for coherent allotriomorphs, material is supposed to be able to add to the entire curved surface; hence the volume diffusivity gives the jump frequency $\tilde{D}/a^2$ and

$$\beta_k = \frac{2\Pi\tilde{D}}{a^4} r^{*2}\bar{C}(1-\cos\theta) \qquad [7]$$

Thus, β_k for coherent allotriomorphs is found to depend on the volume diffusivity and β_k for incoherent allotriomorphs on the boundary diffusivity. Both incubation times and nucleation rates will be strongly influenced since

NUCLEATION KINETICS

In what follows, we are concerned primarily with the nucleation of proeutectoid constituents at grain boundaries in austenite since from the observation of structures of partially transformed steels we know that grain boundary nucleation predominates under a wide variety of conditions. Furthermore, the meticulous metallographic work of Hillert[13] suggests that pearlite attains full cooperation only after an extended period of noncooperative growth, and that the precursor of pearlite is a proeutectoid constituent. If, as is likely, this is generally true, then the nucleation of proeutectoid ferrite or carbide is the proper focal point for this discussion. Since we will be concerned with lower carbon steels, what follows will deal with ferrite.

The discussion of kinetics requires that a detailed model be adopted. We will consider several approaches to this problem in the following section.

In the textbooks,[14] and in the recent literature[15,16] the possibility that nucleation of ferrite is accomplished by the shearing of a small volume of austenite has been discussed. Shewmon[14] clearly distinguishes between a thermally activated event, in which a sharp interface completely bounds the new particle of α, and an event in which the original structure is sheared locally into the product lattice. A theory for ferrite nucleation by shear was put forward by Ryder and Pitsch[16] who assumed that the grain boundary plane remained unrotated during the nucleation event. The theory was shown

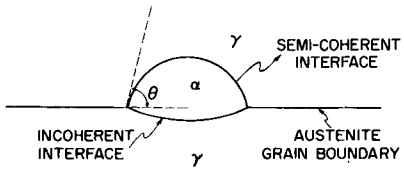

Fig. 9—A schematic semicoherent allotriomorph at the nucleation stage. The nucleus bulges into the parent crystal with which it shares a semicoherent (lower energy) interface.

Table I. Quantities Relevant to the Nucleation of Incoherent and Coherent Allotriomorphs, after Russell[19]

	Incoherent Allotriomorphs	Coherent Allotriomorphs
r^*(radius of critical nucleus)	$2\sigma_{\alpha\beta}/\Delta G_v$	$-2\sigma_{\alpha\beta}/\Delta G_v$
n_k(number of solute atoms)	$\frac{64\Pi\sigma_{\alpha\beta}^3 \hat{C} f(\theta)}{3\Delta G_v^3}$	$\frac{32\Pi\sigma_{\alpha\beta}^3 \hat{C} f(\theta)}{3\Delta G_v^3}$
ΔG^* energy/critical nucleus	$\frac{32\Pi\sigma_{\alpha\beta}^3 f(\theta)}{3\Delta G_v^2}$	$\frac{16\Pi\sigma_{\alpha\beta}^3 f(\theta)}{3\Delta G_v^2}$
τ(incubation time)	$\frac{6kTn_k}{\Delta G_v\beta_k} \alpha \frac{T}{D^b_{\text{eff}}\Delta G_v^3}$	$\frac{6kTn_k}{\Delta G_v^*\beta_k} \alpha \frac{T}{D\Delta G_v^2}$

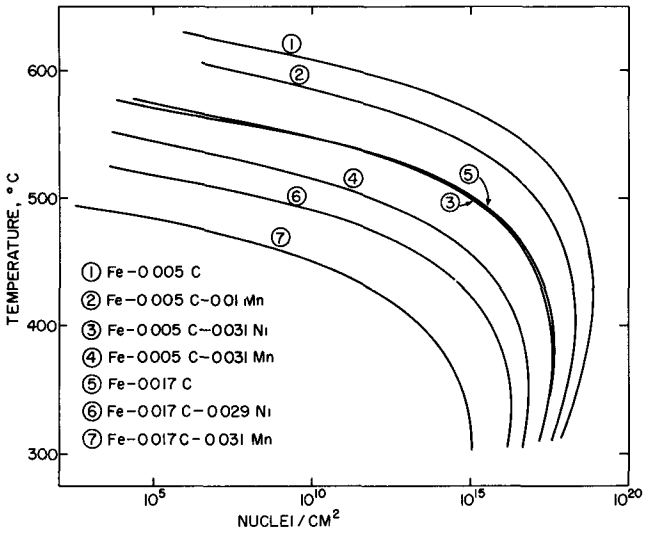

Fig. 10—Nucleation rates calculated for $\sigma_{\alpha\beta} = 75$ ergs/cm^2. β_k is assumed to be determined by boundary diffusion with $D^b_{\text{eff}} = e^{-30{,}600/RT}$. If $\sigma_{\alpha\beta}$ is taken as 100 ergs/cm^2 similar rates are obtained at temperatures about 75°C lower than those shown here.

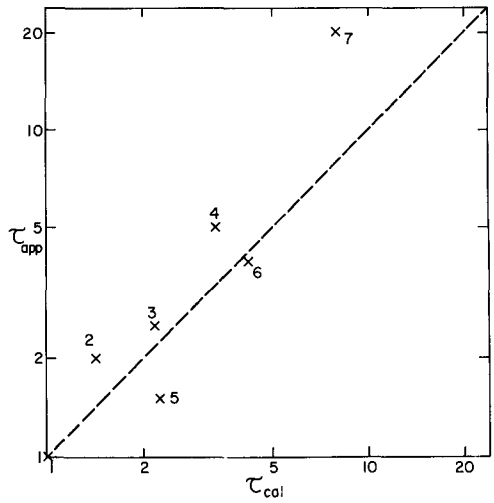

Fig. 11—Comparison of calculated relative incubation times (τcalc) and incubation times estimated from the reaction start times (τapp) on TTT diagrams at 450°C. For this calculation the τapp and τcalc were taken as 1 s for alloy 1 and we have assumed $\tau\alpha(1/\Delta G_v^3)$ (see Table I).

to be consistent with the experimental scatter in orientation relationships (near Kurdjumov-Sachs) found for ferrite allotriomorphs in Fe-C alloys. More recently, Kennon and Purdy[17] analyzed orientation relationships between α and β brass using the Ryder-Pitsch analysis, and showed that this particular theory predicted the experimental scatter of their results, but failed when it was applied to individual precipitates. This observation casts some doubt on the proposition that ferrite nucleates by a shearing process of the type envisioned by Ryder and Pitsch.

Thermally activated incoherent grain boundary nucleation has been discussed by Clemm and Fisher.[18] They assumed that allotriomorphs nucleate as double range of interest. Fortunately, this procedure is comparatively insensitive to the model chosen (*e.g.*, coherent or incoherent nucleation, controlled by interstitial or substitutional volume or boundary diffusion) but is very sensitive to $\sigma_{\alpha\beta}$, especially at low supersaturations. We have chosen to keep $\sigma_{\alpha\beta}$ as high as possible, to be consistent with prior kinetic work[21] which placed the energy of a ferrite boundary (at a Widmanstätten plate tip, and assumed partially coherent) in the neighborhood of 200 ergs per sq cm. Thus we arrive at a "best" value of $\sigma_{\alpha\beta}$ of about 75 ergs per sq cm. Fig. 10 shows several families of rates calculated using this value in our preferred model.

We next inquire into limits on the frequency factor, β_k, as constrained by fundamental processes and by empirical results. As noted above, the reaction start time on a TTT curve is determined by the incubation time, τ, and by the time required for the precipitates to reach observable size. At higher temperatures, rates of nucleation and growth may be low and so both contribute to the time for observable transformation. At 450 to 500°C, however, our calculated rates of nucleation are large for all alloys studied (except the high Mn alloy, number 7) and for all models considered (as noted above). Reference to experiment and to the theory of proeutectoid growth[22,23] suggests that high rates of growth will also exist for this temperature, such that

Table II. Fe-C-X Systems Studies

Alloy No.	At. Pct C	At. Pct Ni	At. Pct Mn
1	0.5	–	–
2	0.5	–	1
3	0.5	3	–
4	0.5	–	3
5	1.7	–	–
6	1.7	3	–
7	1.7	–	3

the times for initiation of reaction on TTT diagrams will be a guide to the magnitude of the incubation time, τ. This was verified by calculations based on the Johnson-Mehl[24] equation as modified by Dubé.[25]

Thus we have, for a limited range of temperature and alloying element levels, an estimate of τ which corresponds to experimental TTT curves. Without inquiring further into the rate-limiting process, we can estimate the isothermal alloying-element effect on the TTT diagrams using the fact that $\tau \propto 1/(\Delta G_v)^3$ for boundary diffusion limited nucleation. Fig. 11 shows the result of comparison with experimental TTT curves.[22,37] For the alloys listed in Table II. Here we have taken $\tau = 1$ s for the binary Fe-0.005 C alloy. The agreement is seen to be generally quite good, and poorest for the high manganese alloy, no. 7, which is expected to possess the lowest rates of nucleation and growth.

$$\tau \propto \frac{Tn_k^2}{\Delta G^* \beta_k} \qquad [8]$$

and the steady state rate of nucleation

$$J \propto \beta_k C_k^0 \qquad [9]$$

where C_k^0, the concentration of critical nuclei, is

$$C_k^0 \equiv \frac{N_0}{\hat{C}} e^{-\Delta G^*/kT} \qquad [10]$$

and N_0 is the number of atoms per unit area of boundary.

ESTIMATION OF THE RELATIVE HARDENABILITY EFFECTS OF ALLOYING ELEMENTS

The equations of the previous section permit us to catalog the fundamental quantities needed to calculated incubation times and nucleation rates: these are the interfacial free energy, $\sigma_{\alpha\beta}$, the effective diffusion coefficient, D_{eff}, and the volume free energy for nucleation, ΔG_v. We begin this discussion with an assumed knowledge of ΔG_v only.

The quantities predicted by the theory (the incubation time τ, and steady state nucleation rate J) are accessible to experiment, but we are aware of no such measurements for simple binary or ternary steels. Therefore, we will focus on the prediction of certain aspects of experimental TTT curves, taking cognizance of available experimental growth data and theoretical models for ferrite growth. It is recognized that, at the very least, the position of the ferrite-start line on a TTT diagram places an upper limit on the incubation time, τ, and requires a corresponding lower limit on the steady state nucleation rate, J.

We will begin by assuming that the free energy for nucleation, at large supersaturation ΔG_v is that calculated on the paraequilibrium model. Therefore, the nucleus and its properties are not appreciably changed by the addition of alloying elements.

Next, we consider the assignment of an optimum value to $\sigma_{\alpha\beta}$. This quantity is unknown, so is adjusted such that sensible nucleation rates are obtained for a wide range of Fe-C and Fe-C-X alloys over the temperature

In the absence of accurate nucleation data, and of accurate activation energies for all possible rate-determining processes, it is difficult to attach a firm value to the activation energy for nucleation. However, using the fact that the incubation time τ must be no larger than the reaction-start times at all temperatures, a theoretical fit to the TTT curves allowed us to place an upper limit of 35,000 cal per mol on this quantity. Higher activation energies would yield too great an incubation time at some temperatures.

Austenite grain size is not considered a major factor in determining reaction start times at lower temperatures. However, since our nucleation rates are given in nuclei per unit area of grain boundary per unit time, a complete TTT diagram calculated using these data would show a grain-size dependence of fraction transformed.

The discussion thus far has been limited to the alloying elements Mn and Ni. However, we submit that the approach taken so far is qualitatively consistent with the known behavior of such elements as Co and Si: as supersaturation is changed by alloying element additions, both nucleation and growth should be influenced in the same way, *i.e.*, accelerated for increased supersaturations, and retarded for decreased supersaturations. Hence the reduction of the reaction start time associated with cobalt additions is understandable.

The calculation procedures used here will only yield hardenability effects which result in a shift of the TTT diagram to the right or left, with little change in the shape of the curve. Also, the magnitude of the shift will be simply related to the change in supersaturation, as reflected in ΔG_v. It is immediately apparent, on this basis, that the bay-forming elements Mo and Cr are anomalous. The effect of a modest addition (say 1 pct of Mo) is to delay selectively the reaction at intermediate temperatures. While the calculated equilibria are admittedly not as certain as those for Ni and Mn, they give no indication of a corresponding major decrease in supersaturation at temperatures where, experimentally, nucleation and/or growth are inhibited. Thus, our calculated nucleation rates remain large for steels containing these elements through the temperature range included by the bay, just as the calculated growth rates of Kinsman and Aaronson[22] (based on a paraequilibrium model) failed to reflect the major inhibition observed in Fe-C-Mo. We have therefore not been successful in rationalizing the behavior of the carbide-forming ferrite stabilizers Mo and Cr, nor have we managed to account for the effect of boron on any reasonable macroscopic thermodynamic model.

This discussion comprises the maximum in quantitative inference in the absence of experimental measurements for simple binary and ternary steels. It appears that the calculations of bulk thermodynamic effects of alloying elements is sufficient for the semiquantitative understanding of the effects of a number of elements but even this simple test of relative effectiveness fails conclusively in the case of strong carbide-forming elements.

A MODEL FOR THE CRITICAL NUCLEUS

Let us now consider a possible form of ferrite nucleus (semicoherent) at a high-angle austenite grain boundary. We expect that the K-S related side will be of low average interfacial free energy. The directions perpendicular to $\langle 111\rangle_\gamma$ should have an energy similar to that estimated for Widmanstätten plate tips by Trivedi et al.,[21] *i.e.*, 200 ergs per sq cm. This is about one quarter of that thought reasonable for austenite grain boundaries ~750 ergs per sq cm. Now it is known that Widmanstätten plates do not tend to spheroidize on prolonged holding at temperature; hence the interface energy is likely to be strongly anisotropic, with the Widmanstätten habit planes possessing very low energies, say one-sixth of the tip energy, or about 30 ergs per sq cm. The character of the interface in this cusp orientation has been the subject of conjecture by a number of writers.

Paxton[26] superimposed $(110)_\alpha$ and $(111)_\gamma$ planar models and noted that isolated regions of good fit were separated by extensive regions of mismatch. More recently, Malcolm[27] observed what appeared to be coherent segments of α-β interface in brass, and Hall *et al.*[28] found that Cr precipitates in Cu were bounded by dislocated interfaces. They showed that, by tilting the interface plane from $\langle 111\rangle_\gamma$, the regions of good fit could be made to include increasingly large fractions of the boundary area, although periodic defective regions are still required. Now the dimensions of the critical nucleus may well be less than the distance between imperfect regions, so that we might expect the interface near $(111)_\gamma$ to be almost completely coherent and to possess a very low energy.

Thus, our model for the nucleus involves a half disc, lying in one grain, with its half-thickness to radius ratio given by $\sigma^e_{\alpha\beta}/\sigma_{\alpha\beta} \sim 0.2$ as required by the equilibrium condition discussed previously. The incoherent boundary energy is expected to be similar to that of the

grain boundary $\sigma_{\beta\beta}$ (Fig. 12). Elementary geometry then gives the disc radius

$$r^* = -2\sigma_2/\Delta G_v \quad [11]$$

and

$$\Delta G^* \propto \frac{\sigma_2^2 \sigma_1}{(\Delta G_v)^2} \quad [12]$$

Thus the average or effective $\sigma_{\alpha\beta}$ is of order 75 ergs per sq cm, the value which was found to be required to generate observable nucleation rates in the previous section. The interpretation of the frequency factor β_k poses a more difficult problem. We must immediately rule out volume diffusion of substitutional elements as a rate-determining step, because the activation energy for this process is too high. (We required < 35,000 cal per mol for the rate-determining step in the previous section).

Carbon volume diffusion is a possible rate-determining factor. However, when we consider the number of carbon atoms that must be rejected from a volume of austenite which corresponds to a typical ferrite critical nucleus containing, say, 200 iron atoms, we find this number is about unity. It therefore seems most unlikely that carbon diffusion will determine nucleation rates. In addition it will generally be possible to find critical nucleus-sized volumes in austenite which are completely free of carbon.

We are thus led to further consideration of the model shown in Fig. 12. The equilibrium condition is expected to hold over the growth of the critical nucleus to the supercritical state. This requires that the shape in Fig. 12 be maintained during growth, which then requires displacement of the planar coherent interfaces. We will postulate that this normal displacement takes place heterogeneously, involving lateral propagation of an incoherent ledge, emanating from the incoherent grain boundary.

The rate of nucleation will then depend on the frequency with which substitutional atoms on the ledge region join the parent crystal. If we assume that this is similar to the boundary jump frequency then the activation energy requirement of the previous section can be met.

While the preceding discussion is highly conjectural, the model has the advantage of being consistent with what is known or generally inferred about interfaces of the kind believed to exist at the *K-S* oriented side of the nucleus, and the β_k extracted is in order-of-magnitude agreement with the observed kinetics of ferrite formation.

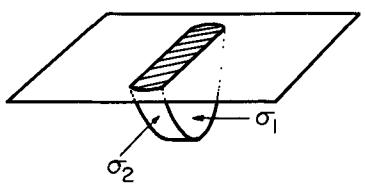

Fig. 12—A model for the disc-shaped semicoherent grain boundary nucleus. The planar sides, of energy σ_1, lie on low energy habit planes in the lower grain and may therefore be inclined to the grain boundary normal. The upper (shaded) boundary is considered to be incoherent, and bulges slightly into the upper grain. The shape of the disc is determined by the relative edge and facet free energies, σ_1 and σ_2, and the effective free energy for the nucleus becomes approximately $(\sigma_1\sigma_2^2)^{1/3}$.

THE ROLE OF CARBIDE-FORMING ELEMENTS

In the previous sections, a simple thermodynamic model was used to estimate incubation times, and to show that carbide-forming elements are not "well-behaved." We will include boron in this group, since it is clear that boron additions at the level commonly used in steels are unlikely to generate the enormous changes in ΔG_v required for the hardenability obtained. We might conjecture that boron (or Cr, or Mo) influence the interfacial energies enough to make this difference. However, it seems unlikely that a surface-active element would reduce the coherent interfacial energy significantly; and there is some experimental evidence that boron reduces the grain-boundary energy by a few percent only.[29]

We will thus consider the possibility (originally suggested by Zener[30] that these elements, when added to steels, result in copious nucleation of alloy carbides, which grow extremely slowly and interfere with ferrite nucleation.

Let us first consider the element boron, which is known to form a borocarbide, of the type $M_{23}C_3B_3$. This phase is cubic and admits of an orientation relationship with austenite which yields a coherent, nearly isotropic interface, very probably of low energy. There is ample evidence that this phase forms at the grain boundaries very early in isothermal treatment (as would be expected from the high diffusion rates of the interstitial solutes, boron and carbon), and thus should act as a heterogeneous nucleation site for proeutectoid ferrite.[31] At first sight one would not look towards a demonstrated heterogeneous nucleation catalyst for a nucleation inhibition mechanism. However, we note that by the time the borocarbide is observed (normally by optical microscopy) considerable coarsening must have occurred, so that a large amount of *continuous* incoherent borocarbide/austenite interface is available to act as a ferrite nucleation site. Thus it is not unreasonable to suggest that, in early stages, the boron constituent acts to inhibit ferrite-nucleation, by covering the grain boundary with coherent particles, as shown in Fig. 13.

The credibility of this mechanism can be reinforced by estimations of nucleation rates and incubation times for the boron constituent. For an interfacial energy (coherent) of about 30 ergs per sq cm, and ΔG_v of 0 to 200 cal per mol, we find incubation times of less than 10^{-2} s, and nucleation rates of $>10^{+15}$ per sq cm per s for most of the temperature range of interest, implying that borocarbide particles will nucleate quickly and copiously to cover the grain boundary area. In a situation like this the grain boundary precipitates cover and replace with coherent interphase boundary segments the high-energy austenite grain boundaries, and so inhibit ferrite or cementite nucleation. Once the period of ini-

Fig. 13—A schematic side view of an array of semicoherent grain boundary allotriomorphs (say $M_{23}B_3C_3$) which acts to prevent nucleation of a subsequent reaction product.

tial growth is replaced by coarsening, or coarsening combined with growth, the configuration will rapidly change to give large areas of continuous incoherent grain or phase boundary (depleted in carbon) where ferrite can readily nucleate. Hence, we have a rationale which accepts the nucleation catalytic effect of the boron constituent at late stages, but which nevertheless invokes the presence of this phase, as coherent allotrimorphs, as a nucleation-inhibiting agent at early times. This hypothesis can, and should be tested by high resolution metallographic observations of boron-containing steels after brief heat treatment.

A similar approach to the explanation of the effects of other "renegade" elements, here typified by chromium and molybdenum, will now be considered. These elements, in sufficient concentrations, produce a "bay" in the TTT diagram. Until the present work, the bay has been postulated to result from a transition from partitioned to unpartitioned growth,[32] or to an impurity drag mechanism[22,23] in which the carbon content at the austenite/ferrite boundary is reduced to that in equilibrium with an alloying-element-enriched boundary region. The first hypothesis, while attractive, has been disproven by microanalytic techniques.[34] The second is current, and remains to be tested. We believe, however, that the impurity (alloying element) will be equally concentrated at the boundary in both the impurity drag and local equilibrium[23,35] cases. Since, in both models, the activity of carbon is taken to vary slowly through the interface, we consider that the impurity drag mechanism exists as an approximate limiting case of the local equilibrium growth model, which always predicts slower growth than the paraequilibrium model,[12,33] but which appears to be inadequate to account for the great inhibition of ferrite formation found here.* [We say "appears to be inadequate" because of real uncertainties in the pertinent equilibria for these α-loop carbide-forming elements]. While we agree with Aaronson *et al.*[10] that the absorption of surface-active elements can indeed alter interfacial energies, and so affect rates of nucleation, we do not believe that most coherent interfacial energies will be much influenced in this way. A reduction of the incoherent grain boundary energy attending impurity absorption would have a small effect on nucleation if the incoherent interphase boundary energy is similarly affected.

*The reader is referred to the previous contribution, by Coates,[7] where these models are explored in detail.

In summary, our current perception is that the impurity drag effect exists, but that it is probably insufficient to account for the nucleation and growth retarding effects of the strong carbide-forming ferrite stabilizers. Thus we are led to present an alternative hypothesis, which is consistent with the carbide-forming tendency of these elements, and which like the impurity drag hypothesis, remains to be tested experimentally.

Coherent grain-boundary carbides containing excess Mo or Cr cannot nucleate in time to interfere with ferrite nucleation, since these elements diffuse much too slowly. It is quite possible, however, that the growth (and to a lesser extent the nucleation) of ferrite in these systems is inhibited at higher temperatures by the formation of precursor clusters, which are enriched in alloying elements (Cr or Mo) and in carbon. Nucleation theory does not apply to the formation of such coherent

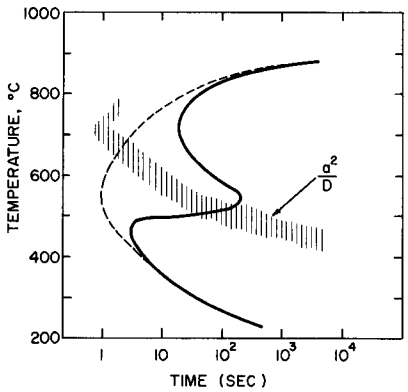

Fig. 14—Illustrating the possible effect of prior clustering of substitutional alloying elements and carbon on a TTT diagram. The time for a cluster growth to a 20Å radius is estimated from $t \simeq a^2/D$, and shown as a shaded curve. Without the precursor clustering reaction the broken line could be obtained. The full curve schematically incorporates the retarding effect of the clustering reaction.

clusters, but the minimum time for clusters to grow to a size sufficient to hinder ferrite formation can be crudely estimated from self-diffusion data for substitutional elements in austenite using a simple $\sqrt{Dt}$ argument. Indeed, it is found that the times for growth to 20Å radius become large at a temperature which coincides with the bay on all such TTT curves, as illustrated in Fig. 14. This would permit the formation of ferrite, at lower temperatures, at rates uninhibited by the clusters.

The drag, or inhibition of ferrite formation, is supposed to arise because carbon must be dissociated from the alloying element clusters if ferrite is to form. Hence an interfacial reaction component is effectively introduced into what was previously a volume diffusion controlled process, and the carbon diffusion potential (and gradient) will be accordingly reduced and growth inhibited. One can think of a number of experiments which can be designed to credit or discredit this idea. It is offered here as a plausible alternative to the impurity drag model, and one which merits further consideration.

CONCLUSION

In preparing this paper, we have become aware of the paucity of experimental information available on such fundamental quantities as nucleation rates and incubation times in high-purity binary and ternary steels. Also, we are just beginning to gain an understanding of the details of the structure of fcc-bcc interfaces. Accordingly, much of what has been put forward here awaits confirmation by carefully designed experiments on appropriate alloy systems.

We can nonetheless conclude that:

1) Classical nucleation theory is sufficiently well-developed for the rationalization of the relative effects of such alloying elements as Mn, Ni, Co on nucleation of ferrite in steels. In the process of rationalization of observed transformation data, we have been led to place limits on the effective interfacial free energy for ferrite nucleation, and on the activation energy of the rate-limiting process. The model proposed here for the ferrite nucleus is not inconsistent with these limits.

2) In the case of carbide-forming ferrite stabilizers, the observed hardenability cannot be attributed simply to thermodynamic factors, and we propose, instead, that precursor reactions interfere with the formation of proeutectoid constituents. Boron additions are conjectured to yield numerous coherent borocarbide grain-boundary precipitates, which interfere with ferrite nucleation when they are first formed (but which catalyze the ferrite reaction after they have coarsened). On the other hand, chromium and molybdenum additions may lead at higher temperatures to the formation of clusters, to which carbon atoms are bound. This suggestion is put forward as a possible reason for the bay in TTT curves, of steels containing these elements. It is to be considered as an alternative to the impurity drag hypothesis.

ACKNOWLEDGMENTS

We are grateful to our colleague, Professor J. S. Kirkaldy, for a critical reading of this manuscript, and to Professor H. I. Aaronson, for valuable discussions. This work was supported by the National Research Council of Canada.

REFERENCES

1. J. N. Hobstetter *Decomposition of Austenite by Diffusional Processes,* V. F. Zackay and H. I. Aaronson, eds., Interscience Publishers, New York, 1962.
2. J. W. Christian *The Theory of Transformations in Metals and Alloys,* Pergamon Press, Oxford, 1965
3. K C. Russell *Phase Transformations,* ASM, 1968.
4. J. W. Cahn and J. E. Hilliard *J of Chem. Phys*, 1959, vol. 32 (3), p. 688
5. J. E. Hilliard *Phase Transformation,* ASM, 1968.
6. M. Hillert *Jernkontorets Ann.,* 1957, vol. 141, p. 757.
7. D. Coates *Met. Trans*, 1973, vol 4, p. 2313.
8. A. Hultgren *Jernkontorets Ann.,* 1951, vol. 135, p 403
9. M. Hillert *Ibid,* 1952, vol. 136, p. 25.
10 H. I. Aaronson, H. A. Domian, and G. M. Pound *Trans. TMS-AIME,* 1966, vol. 236, p. 768.
11 R. C. Sharma McMaster University, Hamilton, Ontario, Canada, unpublished research, 1972.
12 J. B. Gilmour, G. R. Purdy, and J. S. Kirkaldy *Met Trans.,* 1972, vol 3, p. 1455.
13. M. Hillert *Decomposition of Austenite by Diffusional Processes,* V. F. Zackay and H. I. Aaronson, eds., Interscience Publishers, New York, 1962.
14. P. G. Shewmon *Transformations in Metals,* McGraw-Hill Book Co , 1969.
15. P. L. Ryder, W. Pitsch, and R. F. Mehl *Acta Met*, 1967, vol. 15, p. 1431.
16. P. L. Ryder and W. Pitsch *Acta Met.,* 1966, vol 14, p 1437.
17. N. Kennon and G. R. Purdy. McMaster University, Hamilton, Ontario, Canada, unpublished research, 1970.
18. P. J. Clemm and J. C Fisher. *Acta Met.,* 1955, vol. 3, p 70.
19. K. C. Russell *Acta Met*, 1969, vol 17, p. 1123.
20. L. Onsager *Phys. Rev.,* 1931, vol. 37, p. 405.
21 R. Trivedi Ph.D. Thesis, Carnegie Institute of Technology, 1966, as quoted by H. I Aaronson, C Laird, and K. R. Kinsman, Phase Transformations, ASM, 1968.
22. K. R. Kinsman and H. I. Aaronson *Transformation and Hardenability in Steels, Climax Molybdenum,* Ann Arbor, 1967, p. 33.
23. G. R. Purdy, D. H. Weichert, and J. S Kirkaldy *Trans. TMS-AIME,* 1964, vol. 230, p. 1025.
24. W. A. Johnson and R. F. Mehl *Trans. TMS-AIME,* 1939, vol. 135, p. 416.
25. C. A. Dube Ph.D. Thesis, Carnegie Institute of Technology, 1948.
26. H. W. Paxton· *J. Chem. Phys.,* 1957, vol. 26, p. 1769.
27 J. A. Malcolm and G. R. Purdy *Trans. TMS-AIME,* 1967, vol. 239, p. 1391.
28. M. G. Hall, H. I. Aaronson, and K. R. Kinsman *Surface Science,* 1972, vol. 31, p. 257.
29. A. M. Adair, J. W. Spretnak, and R. Speiser *Trans. TMS-AIME,* 1955, vol 203, p. 353.
30. C. Zener *Trans. TMS-AIME,* 1946, vol. 167, p. 550.
31 G. F. Melloy, P. R. Slimmon, and P. P. Podgursky *Met Trans.,* 1973, vol. 4, p. 2279
32. A. Hultgren *Trans. ASM,* 1947, vol. 39, p. 915.
33. M Hillert *The Mechanism of Phase Transformations in Crystalline Solids,* Inst. of Metals, Monograph No. 33, 1969, p. 331.
34. H. I. Aaronson *Trans. TMS-AIME,* 1962, vol. 224, p. 870.
35. J. Tiley M. Eng. Thesis, McMaster University, 1972.
36. H I. Aaronson Michigan Technological University, Houghton, Michigan, private communication, 1972.
37 H. I. Aaronson and H. A. Domian *Trans. TMS-AIME,* 1966, vol. 236, p. 781.